Revisiting Image Vignetting Correction by Constrained Minimization of log-Intensity Entropy

Laura Lopez-Fuentes, Gabriel Oliver, and Sebastia Massanet

Dept. Mathematics and Computer Science, University of the Balearic Islands
Crta. Valldemossa km. 7,5, E-07122 Palma de Mallorca, Spain
llopezfuentes@hotmail.com,goliver@uib.eu,s.massanet@uib.es

Abstract. The correction of the vignetting effect in digital images is a key pre-processing step in several computer vision applications. In this paper, some corrections and improvements to the image vignetting correction algorithm based on the minimization of the log-intensity entropy of the image are proposed. In particular, the new algorithm is able to deal with images with a vignetting that is not in the center of the image through the search of the optical center of the image. The experimental results show that this new version outperforms notably the original algorithm both from the qualitative and the quantitative point of view. The quantitative measures are obtained using an image database with images to which artificial vignetting has been added.

Keywords: Vignetting, entropy, optical center, gain function.

1 Introduction

Vignetting is an undesirable effect in digital images which needs to be corrected as a pre-processing step in computer vision applications. This effect is based on the radial fall off of brightness away from the optical center of the image. Specially, those applications which rely on consistent intensity measurements of a scene are highly affected by the existence of vignetting. For example, image mosaicking, stereo matching and image segmentation, among many others, are applications where the results are notably improved if some previous vignetting correction algorithm is applied to the original image.

There are three types of vignetting according to their cause [1]: natural vignetting, pixel vignetting and mechanical vignetting. Natural vignetting is caused by light reaching different locations on the camera sensor at different angles and is most significant with wide angle lenses. On the other hand, pixel vignetting only affects digital cameras and is caused by angle-dependence of the digital sensors. Mechanical vignetting is an abrupt vignetting which only appears in the corners of the image and is caused by the occlusion by objects entering the camera field of view. Most of the proposed vignetting correction algorithms

are designed to correct the gradual and continuous natural and pixel vignettings since the mechanical one can often be eliminated by using a longer focal length.

There exist basically two different approaches to correct vignetting. The first one lies on the use of multiple images of the same scene at different angles which need to be stitched into a single one, panoramic image. If vignetting affects these images, when the border of an image is superposed on the center of the neighbouring image, the differences of intensities are significant obtaining a poor panoramic image. Some vignetting correction algorithms handle this problem (see [2,3]). However, there exists a second approach which is the vignetting correction based on a single input image from a non-predetermined camera. This problem setting leads to a research that is more useful in practice because it does not require an explicit calibration step or an image sequence as input. Nevertheless, single-image vignetting correction is a challenging problem to solve since the resulting algorithm needs to differentiate the global brightness variations caused by vignetting from those caused by textures or lighting.

This second approach has only been recently studied and some single-image vignetting correction methods have been proposed in the literature. First, Zheng et al. in [4] proposed a method based on a segmentation of the image into regions and a posterior fitting of vignetting functions to the image intensities within these regions. After that, again Zheng et al. in [5] presented a new method that uses the observed symmetry of radial gradient distributions in natural images. Another method, which is designed for microscopy images, was proposed by Leong et al. in [6]. There, the authors smooth the whole image with a Gaussian kernel to eliminate image structure and retain only the low-frequency intensity vignetting field. Other vignetting correction methods can be seen in [7,8,9,10].

In addition to the previous algorithms, in an unpublished article [11], a novel method for single-image vignetting correction through the constrained minimization of log-intensity entropy was proposed. The author applies the concept of information minimization to vignetting correction and uses a constrained radial polynomial vignetting function to correct the effect. The method proves to be faster and more accurate than Zheng's method based on the symmetry of radial gradient distributions [5], which is often used as the comparison benchmark. However, from our point of view, the method presents some mathematical inaccuracies which cause some undesired results and jeopardize the validity of the method. In spite of these technical problems, the underlying idea of the method is interesting and therefore, in this article, we will propose a new version of this algorithm fixing the technical problems of the original version. Furthermore, we will also add an improvement based on the search of the optical center of the image before applying the vignetting correction algorithm. In [11] as well as in most of the vignetting correction methods, the optical center of the image is supposed to be at the center of the image. However, in practice the optical center may lie at a considerable distance from the image center [12] and in such cases,

the actual image optical center needs to be determined for accurate removal of vignetting effects.

The paper is organized as follows. First, in Section 2, the actual single-image vignetting correction based on the minimization of the log-intensity entropy will be recalled. In the next section, we will present the corrected and improved version of the algorithm. In Section 4, some comparison experiments will be carried out to check the performance of our proposal with respect to the original algorithm and Zheng's algorithm [5]. Finally, we end the paper with a section devoted to conclusions and the future work we want to develop.

2 Log-Intensity Entropy Minimization Algorithm

As we have already commented in the introduction, T. Rohlfing proposed in [11] a vignetting correction algorithm based on the constrained minimization of the log-intensity entropy. The algorithm relies on a method developed in [13] where the authors proved that the entropy of an image can be considered as an adequate optimization criterion for the model-free correction of shading artifacts and for microscopy image shading correction. The main hypothesis of that method is that the homogeneous objects have homogeneous intensities which correspond to a single peak and low entropy histogram. On the other hand, if there exists some gradual change of the intensity, as the one caused by vignetting, the peak of the histogram would not be as sharp as before and additional information would be added with an increment of the entropy. Thus, in order to reduce and correct this spatially varying intensity bias the minimization of the entropy becomes necessary.

At this point, for the sake of completeness and in order to fully understand the corrections and improvements that will be made to this algorithm in Section 3, let us recall the main steps of the original version. We refer the reader to [11] for further details. To correct vignetting from the image, Rohlfing's algorithm uses a sixth grade polynomial gain function g which depends on the distance from the image center to the pixel being treated. Specifically,

$$g_{a,b,c}(r) = 1 + ar^2 + br^4 + cr^6$$

where

$$r = \frac{\sqrt{(i-\bar{i})^2 + (j-\bar{j})^2}}{\sqrt{\bar{i}^2 + \bar{j}^2}},$$

(i, j) is whichever pixel from the image and $(\bar{i}, \bar{j})$ is the image center. Therefore we have a function which depends on three real parameters a, b and c, verifying that $g(0)$ corresponds to the image center and $g(1)$ corresponds to the image corners. Once the gain function has been calculated it is multiplied by the original function, obtaining in this way an image with reduced vignetting. Namely,

$$\text{Final image}(i, j) = \text{Original image}(i, j) g_{a,b,c}(r).$$

Obviously, not all the values of the parameters a, b and c generate suitable vignetting correction functions. The vignetting effect is increasing as we move to the borders of the image and consequently, this function g must be strictly increasing for all $0 < r < 1$. In [11], the author determines that the function g will be strictly increasing if, and only if, the parameters satisfy one of the following conditions

$$\begin{aligned}
&C_1 = (c \geq 0 \wedge 4b^2 - 12ac < 0),\\
&C_2 = (c \geq 0 \wedge 4b^2 - 12ac \geq 0 \wedge q_- \leq 0 \wedge q_+ \leq 0),\\
&C_3 = (c \geq 0 \wedge 4b^2 - 12ac \geq 0 \wedge q_- \geq 0 \wedge q_+ \geq 0),\\
&C_4 = (c < 0 \wedge q_- \leq 0 \wedge q_+ \geq 0),\\
&C_5 = (c < 0 \wedge q_- \geq 0 \wedge q_+ \leq 0),
\end{aligned}$$

where q_+ and q_- are defined as

$$q_+ = \frac{-2b + \sqrt{4b^2 - 12ac}}{6c}, \quad q_- = \frac{-2b - \sqrt{4b^2 - 12ac}}{6c}. \tag{1}$$

The criterion for the determination of the optimal values of a, b and c among the ones which satisfy one of the above conditions was established as the minimization of the log-intensity entropy. Let us recall this concept. First, the luminance values $L = \{0, \ldots, 255\}$ are mapped to N histogram bins i using the function $i : L \to \mathbb{R}^+$ given by

$$i(L) = (N-1)\frac{\log(1+L)}{\log 256}.$$

Then the histogram bins n_k are computed using the following formula:

$$n_k = \sum_{\substack{x,y:\\ \lfloor i(L(x,y)) \rfloor = k}} (1 + k - i(L(x,y))) + \sum_{\substack{x,y:\\ \lceil i(L(x,y)) \rceil = k}} (k - i(L(x,y))) \tag{2}$$

At this point, to account for gaps in the image intensity distribution that can appear when scaling quantized data, the histogram is smoothed using a Gaussian kernel G_σ with standard deviation σ: $\hat{\mathbf{n}} = \mathbf{n} \star G_\sigma$. At this point, the discrete entropy is computed as

$$H = \sum_k \hat{p}_k \log \hat{p}_k \tag{3}$$

where $\hat{p}_k = \dfrac{\hat{n}_k}{\sum_j \hat{n}_j}$.

Finally, a hill climbing optimization algorithm is implemented to search in $\mathbb{R}^3$ among those triplets satisfying one of the conditions C_1-C_5 the optimal values (a, b, c) which minimize the log-intensity entropy H. Starting from $(0, 0, 0)$, each one of the parameters is increased and diminished independently by $\delta > 0$. From these 6 triplets, we compute the entropy of the cases satisfying one of the conditions and we update the optimal (a, b, c) to the one with the lowest entropy

(a) Original image with vignetting
$H = 2.0643$

(b) Output of Rohlfing's algorithm
$H = 1.9127$

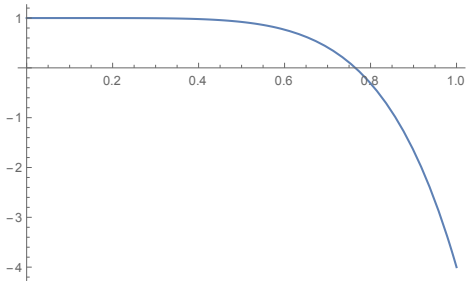

(c) Gain function g

Fig. 1: Undesired behaviour of the original algorithm based on the constrained minimization of the log-intensity [11].

value. When none improves the entropy, δ is reduced by a factor $0 < k < 1$ and the process is repeated. If a new minimum value is achieved, δ is reset to its initial value. Otherwise, we continue reducing δ until we reach a prefixed value δ_0.

3 A Corrected and Improved Algorithm

In this section, we will take a closer look to Rohlfing's algorithm and we will prove that it suffers from some mathematical inaccuracies that cause it to provide some undesired results with some images. As a matter of example, consider the triplet $a = b = 0$ and $c = -5$ which generates the gain function $g(r) = 1 - 5r^6$ which is clearly a strictly decreasing function as can be seen in Figure 1-(c). Note that this function satisfies conditions C_4 and C_5 but although it may reduce the entropy when it is applied to an image with high vignetting as in Figure 1-(a), it increases in fact the vignetting, darkening the whole image.

In addition to the previous problem, an exhaustive analysis of the conditions C_1-C_5 allows to deduce that some cases have been omitted and some others are not well-defined. Note that conditions C_2 and C_3 have non sense when $c = 0$ since q_+ and q_- cannot be defined. Therefore and with the aim to fully determine all the cases leading to suitable gain functions, let us correct these mistakes. Consider the gain function $g_{a,b,c}(r) = 1 + ar^2 + br^4 + cr^6$. To obtain a strictly increasing function, the first derivative must satisfy

$$g'(r) = 2ar + 4br^3 + 6cr^5 > 0$$

for all $0 < r < 1$. Since $r > 0$ and changing $r^2 = q$ we obtain the following inequality

$$a + 2bq + 3cq^2 > 0$$

for all $0 < q < 1$. Thus, the problem is reduced to study this general polynomial. It can be easily checked that this inequality holds if, and only if, one of the following nine conditions on the parameters holds:

[Horizontal positive line]	$C_1 = (a > 0 \wedge b = c = 0)$,
[Increasing line with non-positive root]	$C_2 = (a \geq 0 \wedge b > 0 \wedge c = 0)$,
[Decreasing line with root ≥ 1]	$C_3 = (c = 0 \wedge b < 0 \wedge -a \leq 2b)$,
[Convex parab. without roots]	$C_4 = (c > 0 \wedge b^2 < 3ac)$,
[Convex parab., only one non-positive root]	$C_5 = (c > 0 \wedge b^2 = 3ac \wedge b \geq 0)$,
[Convex parab., only one root ≥ 1]	$C_6 = (c > 0 \wedge b^2 = 3ac \wedge -b \geq 3c)$,
[Convex parab., non-positive highest root]	$C_7 = (c > 0 \wedge b^2 > 3ac \wedge q_+ \leq 0)$,
[Convex parab., lowest root ≥ 1]	$C_8 = (c > 0 \wedge b^2 > 3ac \wedge q_- \geq 1)$,
[Concave parab., lowest root ≤ 0, highest root ≥ 1]	$C_9 = (c < 0 \wedge b^2 > 3ac \wedge q_+ \geq 1 \wedge q_- \leq 0)$,

(4)

where q_+ and q_- are the roots of the polynomial given by Equations (1).

Once the conditions have been corrected, the algorithm does not obtain undesired results. However, as the original version of the algorithm, the method supposes the optical center of the image to be at the center of the image. This assumption leads to applying the gain function g from the center of the image $r = 0$ to the borders $r = 1$. However, it was shown in [12] that the optical center may not coincide with the center of the image and in fact, it could be quite displaced. Thus, it would be necessary to look for the optical center in order to compute the radial distance r of a pixel from the optical center rather than from the center of the image. Several techniques have been proposed for optical center estimation. Some estimate the optical center by locating the radial lens distortion [14] or the vanishing point [15], among other strategies. In this article, we will use a simple approach based on two steps. First, a low-pass Gaussian filter is applied to the image in order to extract the luminance pattern of the image. If the standard deviation of the Gaussian filter is very high, the objects and the structures of the image are removed or smoothed and the obtained image provides an estimation of the shading and luminance pattern of the original

image. After that, we compute the center of mass CM of the image I using the following formula:

$$CM = \left(\frac{\sum\limits_{\substack{1 \le i \le N \\ 1 \le j \le M}} i \cdot I(i,j)}{\sum\limits_{\substack{1 \le i \le N \\ 1 \le j \le M}} I(i,j)}, \frac{\sum\limits_{\substack{1 \le i \le N \\ 1 \le j \le M}} j \cdot I(i,j)}{\sum\limits_{\substack{1 \le i \le N \\ 1 \le j \le M}} I(i,j)} \right) \tag{5}$$

where I is a $N \times M$ image. In Figure 2, we can see how this method is able to detect the optical center of the image when it is not located at the center of the image. Now, we can modify the computation of the radial distance r to account for the optical center located in $CM = (CM_1, CM_2)$ by

$$r = \frac{\sqrt{(x - CM_1)^2 + (y - CM_2)^2}}{\max\limits_{(v_1, v_2)\ \text{vertex}} \sqrt{(v_1 - CM_1)^2 + (v_2 - CM_2)^2}}. \tag{6}$$

Fig. 2: Computation of the center of mass as the optical center of the image. Red: optical center; Blue: center of the image.

To sum up, in Algorithm 1, we have included for a quick view the pseudo-code of the proposed algorithm, where the log-intensity entropy is computed using Equation (3).

In Figure 3, we include a graphical example of how the minimization of the log-intensity entropy helps to correct the vignetting present in an image. While the presence of vignetting reduces the peak of the histogram, the algorithm is able to correct it and get an image, quite similar to the original one.

To end this section, in Figure 4, we include a visual example of the intermediate images obtained by the algorithm including the values of the log-intensity entropy and the triplet (a, b, c) used to correct it. Note that the image is progressively improved while the log-intensity entropy values decrease.

Algorithm 1: Proposed vignetting correction algorithm.

Input: I image with vignetting
Output: F corrected image

Initial values $(a, b, c) = (0, 0, 0)$, $\delta = 8$, $H_{\min} = \text{log-entropy}(I)$, $F = I$;
Compute CM using Equation (5) and r using Equation (6);
while $\delta > \frac{1}{256}$ **do**
    $v_1 = (a + \delta, b, c), v_2 = (a - \delta, b, c), v_3 = (a, b + \delta, c)$;
    $v_4 = (a, b - \delta, c), v_5 = (a, b, c + \delta), v_6 = (a, b, c - \delta)$;
    $H = \min_{vi \text{ satisfies } C_1 \cup \ldots \cup C_9} \text{log-entropy}(I \cdot g_{a,b,c}(r))$;
    if $H < H_{\min}$ **then** $H_{\min} = H$, $F = I \cdot g_{a,b,c}(r)$ for the corresponding v_i;
    $\delta = 8$, $(a, b, c) = v_i$ found;
    else
        $\delta = \frac{\delta}{2}$;

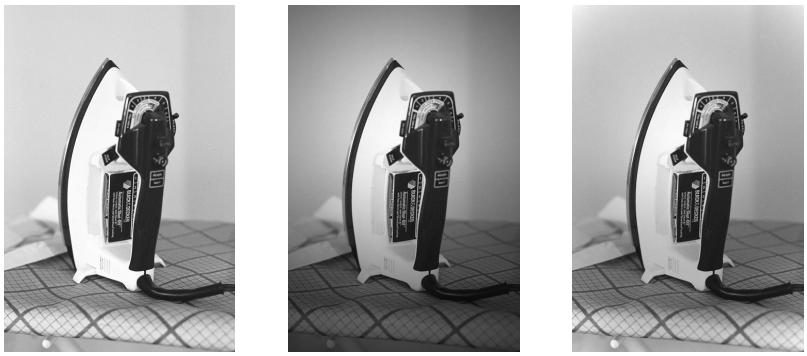

(a) Original image (b) Image with vignetting (c) Corrected image

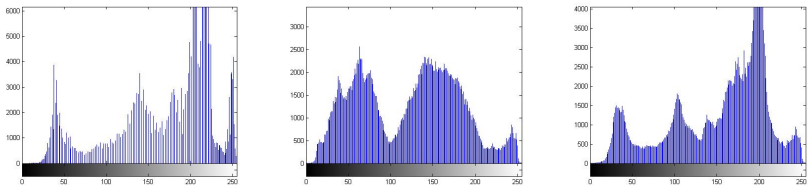

(d) Histogram original image (e) Histogram image with vignetting (f) Histogram corrected image

Fig. 3: Correction of the histogram of the image with vignetting after applying the proposed algorithm.

(a) Original image (b) Image with vignetting (c) Step 1 (d) Step 2

(e) Step 3 (f) Step 5 (g) Step 8 (h) Corrected image

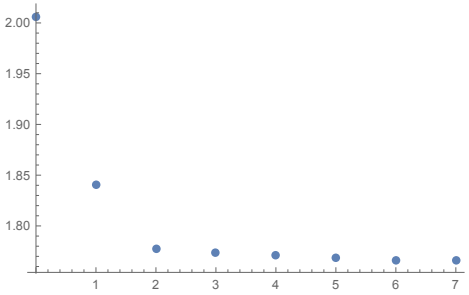

(i) Entropy values

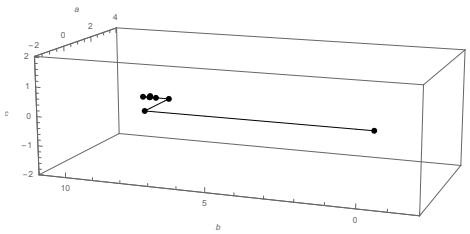

(j) Evolution of (a, b, c) values from $(0, 0, 0) \rightarrow (2.0625, 8.75, 0.0313)$

Fig. 4: Intermediate obtained images using the proposed algorithm and the evolution of the log-intensity entropy values and (a, b, c) triplets.

4 Experimental Results

In this section, we will check the performance of the vignetting correction algorithm proposed in Section 3 with respect to:

1. Rohlfing's algorithm [11], including the corrections on the conditions but without the optical center search,
2. Zheng's algorithm [5], which is often used as a benchmark algorithm in vignetting correction.

All the computations has been carried out using MATLAB R2014a. We have used the implementation of the Zheng's algorithm available in [16], made by the same author and using the default parameter values.

The comparison have been made both from the visual point of view of the results and using objective quantitative performance measures. Nowadays, it is well-established in the literature that the visual inspection of the images obtained by several vignetting correction algorithms can not be the unique criterion with the aim of proving the superiority of one method with respect to the others. This is because each expert has different criteria and preferences and consequently, the reviews given by two experts can differ substantially. For this reason, the use of objective performance measures is growing in popularity to compare the results obtained by different vignetting correction algorithms. However, in order to be able to use some measures, we need an image database that includes for each image with vignetting, the corresponding original image without vignetting.

4.1 Image database

The use of a quantitative measure to compare the output images of different methods implies the availability of a reference image to which compare the results obtained by the different algorithms. This reference image is considered as the perfect image that the algorithms should obtain. For vignetting correction purposes, the reference image must be an image without vignetting. For this reason, the addition of artificial vignetting to natural images with no visible vignetting is a reasonable way to obtain a suitable image database to use in this comparison setting.

We have chosen the first 15 images of the dataset of the University of South Florida[1] ([17]). The image dataset contains indoor and outdoor scenes, and natural and man-made objects. Each of the images contains a single object approximately centred in the image, appearing unoccluded and set against a natural background for the object. Some images have highlights, reflections or low resolution and a visual inspection has been performed to check the absence of vignetting. From these images, we have generated a new database adding artificial vignetting to these images using a simplified version of the Kang-Weiss model (see [18]). Let $A(r)$ be the off-axis illumination factor which is given by

$$A(r) = \frac{1}{\left(1 + \left(\frac{r}{f}\right)^2\right)^2}$$

where f is the effective focal length of the camera and r is the radial distance to the origin point where the factor is applied. Using this factor, the image with vignetting V from an image I is obtained by $V(i,j) = I(i,j) \cdot A(r)$. As the origin point where the factor is applied, we have randomly chosen a point located in the subimage from $\frac{N}{4}$ to $\frac{3N}{4}$ of width and from $\frac{M}{4}$ to $\frac{3M}{4}$ of height of the $N \times M$ image. Thus, the optical center of the image and the center of the image differ in

[1] This image dataset can be downloaded from `ftp://figment.csee.usf.edu/pub/ROC/edge_comparison_dataset.tar.gz`

general. Different values of $f = \{200, 300, 400, 500, 1000\}$ have been considered for the 15 images, generating 75 vignetting images.

4.2 Objective measures

In addition to the visual comparison of the corrected images obtained by the algorithms, the performance will be quantitatively measured by two widely used performance objective measures, namely PSNR and SSIM. Let I_1 and I_2 be two images of dimensions $N \times M$. In the following, we suppose that I_1 is the original vignetting-free image and I_2 is the restored image for which some vignetting correction algorithm has been applied. The peak signal-to-noise ratio (PSNR) is defined by

$$PSNR(I_2, I_1) = 10 \log_{10} \left(\frac{R^2}{MSE(I_2, I_1)} \right) \tag{7}$$

where R is the maximum fluctuation in the input image and MSE is the mean-squared error computed using the following expression:

$$MSE(I_2, I_1) = \frac{\sum_{\substack{1 \le i \le N \\ 1 \le j \le M}} \left(I_2(i,j) - I_1(i,j) \right)^2}{N \times M}. \tag{8}$$

On the other hand, the structural similarity index measure (SSIM) was introduced in [19] under the assumption that human visual perception is highly adapted for extracting structural information from a scene. The measure is defined as follows:

$$\mathrm{SSIM}(I_2, I_1) = \frac{(2\mu_1\mu_2 + C_1)}{(\mu_1^2 + \mu_2^2 + C_1)} \cdot \frac{(2\sigma_{12} + C_2)}{(\sigma_1^2 + \sigma_2^2 + C_2)}, \tag{9}$$

where for $k = 1, 2$, μ_k and σ_k^2 are the mean and the variance of each image, σ_{12} is the covariance between the two images, $C_1 = (0.01 \cdot 255)^2$ and $C_2 = (0.03 \cdot 255)^2$. Larger values of PSNR and SSIM ($0 \le SSIM \le 1$) are indicators of better capabilities for vignetting correction.

4.3 Comparison results

We have applied the three considered vignetting correction algorithms to each vignetting image and we have obtained the values for the two considered objective measures comparing the output to the original free-vignetting image. The results grouped according to the focal length f used to generate the image with vignetting are shown in Tables 1 and 2. As it can be seen, the proposed method outperforms the other methods severely, specially for low values of f which correspond to high levels of vignetting. Note also that the proposed algorithm and Rohlfing's one improve always the images from the quantitative point of view, obtaining better values of the measures with respect to the images with vignetting.

f	PSNR Results							
	Vignetting		Zheng		Rohlfing		Proposed	
	Mean	σ	Mean	σ	Mean	σ	Mean	σ
200	8.0352	2.1118	7.9633	2.0659	9.5656	2.8170	12.2968	3.1512
300	10.0883	2.2567	10.0994	2.1933	10.9610	2.6213	13.0706	3.2286
400	12.8669	2.3230	13.0135	2.2496	15.5541	3.2876	17.2203	4.0243
500	14.3902	2.7940	14.5138	2.8246	16.5148	3.9082	16.9943	3.3770
1000	23.4953	3.1797	22.5514	3.1464	24.6718	3.3896	25.2753	3.6489

Table 1: Mean and standard deviation of the PSNR values obtained by the vignetting correction methods according to the value of f.

f	SSIM Results							
	Vignetting		Zheng		Rohlfing		Proposed	
	Mean	σ	Mean	σ	Mean	σ	Mean	σ
200	0.3736	0.0558	0.3479	0.0609	0.5108	0.1541	0.7034	0.1018
300	0.5693	0.0497	0.5621	0.0526	0.6252	0.0636	0.7350	0.0868
400	0.7305	0.0520	0.7352	0.0539	0.8019	0.0692	0.8499	0.0481
500	0.8034	0.0364	0.8072	0.0382	0.8437	0.0451	0.8628	0.0291
1000	0.9158	0.0184	0.9120	0.0170	0.9194	0.0171	0.9212	0.0175

Table 2: Mean and standard deviation of the SSIM values obtained by the vignetting correction methods according to the value of f.

In Figure 5, some results are displayed comparing the output of the different algorithms. The proposed algorithm is able to reduce the vignetting even if the original image is corrupted by high amounts of it. Note that Zheng's algorithm gives results which although reducing somewhat the amount of vignetting, it changes completely the tone of the image, darkening it, specially for higher amounts of vignetting. Another conclusion which emerges from the images in the first two rows, in which vignetting is very off-centred, is the capability of the step included in the proposed algorithm to detect the optical center of the image. While the proposed algorithm applies the gaining function with origin at the optical center, Rohlfing's algorithm applies it at the center of the image being unable to reduce the vignetting uniformly in the whole image.

5 Conclusions and Future Work

Single-image vignetting correction is a useful technique to avoid the need of the calibration of the camera or the disposal of several images to correct vignetting. In this paper, we have deeply analysed the vignetting correction algorithm based on the minimization of the log-intensity entropy of the image, that was proposed in [11]. We have proved that the algorithm had several mathematical inaccura-

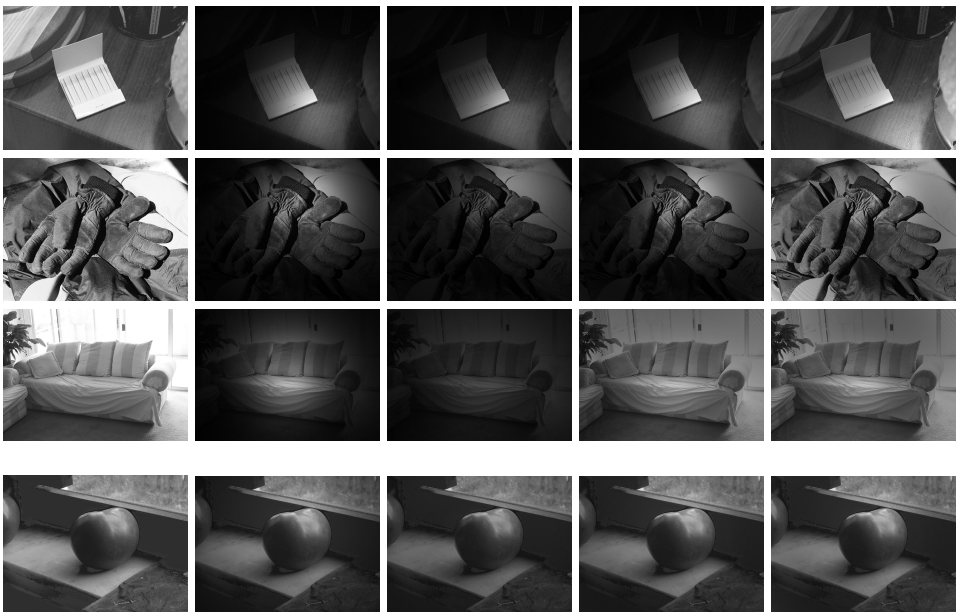

(a) Free vignetting (b) Vignetting (c) Zheng's (d) Rohlfing (e) Proposed

Fig. 5: Comparison of the outputs of the different vignetting correction algorithms for several images.

cies which caused to perform inappropriately in several images. Here, we have corrected these mistakes and we have proposed a revised version of the algorithm adding the improvement of the search of the optical center of the image to handle adequately images with off-centred vignetting. The comparison results ensure the potential of this algorithm from both the visual and the quantitative point of view.

As a future work, we want to generalize our algorithm to deal with color images and with images having more than one focus of vignetting. These last images correspond to images obtained using several illumination focuses.

Acknowledgement

This paper has been partially supported by the Spanish Grants TIN2013-42795-P and DPI2011-27977-C03-3.

References

1. S.F. Ray. *Applied Photographic Optics: Lenses and Optical Systems for Photography, Film, Video, Electronic and Digital Imaging.* Focal, 2002.

2. D.B. Goldman. Vignette and exposure calibration and compensation. *IEEE Transactions on Pattern Analysis and Machine Intelligence*, 32(12):2276–2288, 2010.
3. J. Jia and C.-K. Tang. Tensor voting for image correction by global and local intensity alignment. *IEEE Transactions on Pattern Analysis and Machine Intelligence*, 27:36–50, 2005.
4. Y. Zheng, S. Lin, C. Kambhamettu, J. Yu, and S. B. Kang. Single-image vignetting correction. *IEEE Transactions on Pattern Analysis and Machine Intelligence*, 31(12):2243–2256, 2009.
5. Y. Zheng, J. Yu, S. B. Kang, S. Lin, and C. Kambhamettu. Single-image vignetting correction using radial gradient symmetry. In *IEEE Computer Society Conference on Computer Vision and Pattern Recognition (CVPR 2008), 24-26 June 2008, Anchorage, Alaska, USA*, pages 1–8. IEEE Computer Society, 2008.
6. F. J. W-M. Leong, M. Brady, and J. O'D. McGee. Correction of uneven illumination (vignetting) in digital microscopy images. *Journal of Clinical Pathology*, 56(8):619–621, 2003.
7. Y. Zheng, S. Lin, S. B. Kang, R. Xiao, J. C. Gee, and C. Kambhamettu. Single-image vignetting correction from gradient distribution symmetries. *IEEE Trans. Pattern Anal. Mach. Intell.*, 35(6):1480–1494, 2013.
8. W. Yu, Y. Chung, and J. Soh. Vignetting distortion correction method for high quality digital imaging. In *Proceedings of the 17th International Conference on Pattern Recognition, 2004. ICPR 2004.*, volume 3, pages 666–669, 2004.
9. K. He, P.-F. Tang, and R. Liang. Vignetting image correction based on gaussian quadrics fitting. In *Fifth International Conference on Natural Computation, 2009. ICNC '09.*, volume 5, pages 158–161, 2009.
10. H. Cho, H. Lee, and S. Lee. Radial bright channel prior for single image vignetting correction. In D. Fleet et al., editor, *Computer Vision, ECCV 2014*, volume 8690 of *Lecture Notes in Computer Science*, pages 189–202. Springer, 2014.
11. T. Rohlfing. Single-image vignetting correction by constrained minimization of log-intensity entropy. Unpublished, 2012.
12. R.K. Lenz and R.Y. Tsai. Techniques for calibration of the scale factor and image center for high accuracy 3-D machine vision metrology. *IEEE Transactions on Pattern Analysis and Machine Intelligence*, 10(5):713–720, 1988.
13. B. Likar, J. B. Maintz, M. A. Viergever, and F. Pernus. Retrospective shading correction based on entropy minimization. *Journal of Microscopy*, 197(3):285–295, 2000.
14. R. Willson. *Modeling and Calibration of Automated Zoom Lenses*. PhD thesis, Robotics Institute, Carnegie Mellon University, Pittsburgh, PA, 1994.
15. L.-L. Wang and W.-H. Tsai. Computing camera parameters using vanishing-line information from a rectangular parallelepiped. *Machine Vision and Applications*, 3(3):129–141, 1990.
16. Y. Zheng. Matlab Central - nu_corrector, May 2010. http://www.mathworks.com/matlabcentral/fileexchange/27315-nu-corrector.
17. K. Bowyer, C. Kranenburg, and S. Dougherty. Edge detector evaluation using empirical ROC curves. In *IEEE Conf. on Computer Vision and Pattern Recognition (CVPR '99)*, volume 1, pages 354–359, 1999.
18. S. Kang and R. Weiss. Can we calibrate a camera using an image of a flat, textureless Lambertian surface? In D. Vernon, editor, *Computer Vision, ECCV 2000*, volume 1843 of *Lecture Notes in Computer Science*, pages 640–653. Springer, 2000.
19. Z. Wang, A. C. Bovik, H. R. Sheikh, and E. P. Simoncelli. Image quality assessment: From error visibility to structural similarity. *IEEE Transactions on Image Processing*, 13(4):600–612, 2004.